Electronic Supplementary Material (ESI) for Journal of Materials Chemistry C

Supplementary Information

Structurally simple thienodipyrandione-containing reversible fluorescent switching piezo- and acido-chromic materials

*Rajeswara Rao M, Chia-Wei Liao and Shih-Sheng Sun**

Content

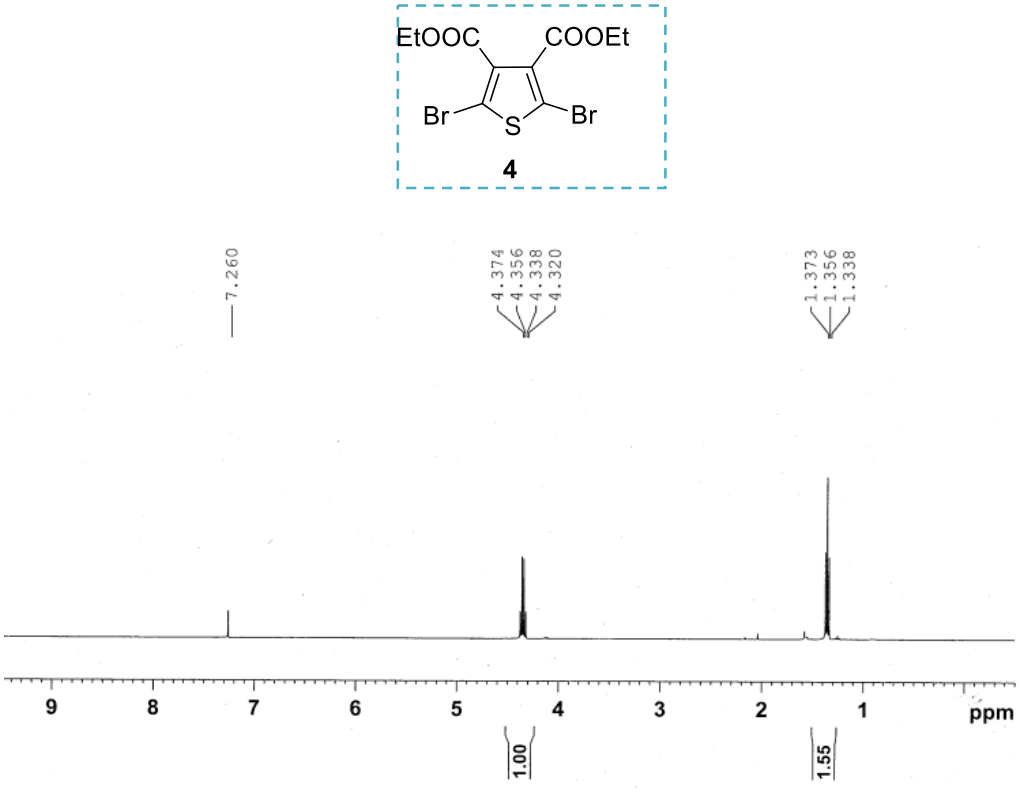

Figure S1: ^{1}H NMR spectrum of compound **4** in $CDCl_3$.

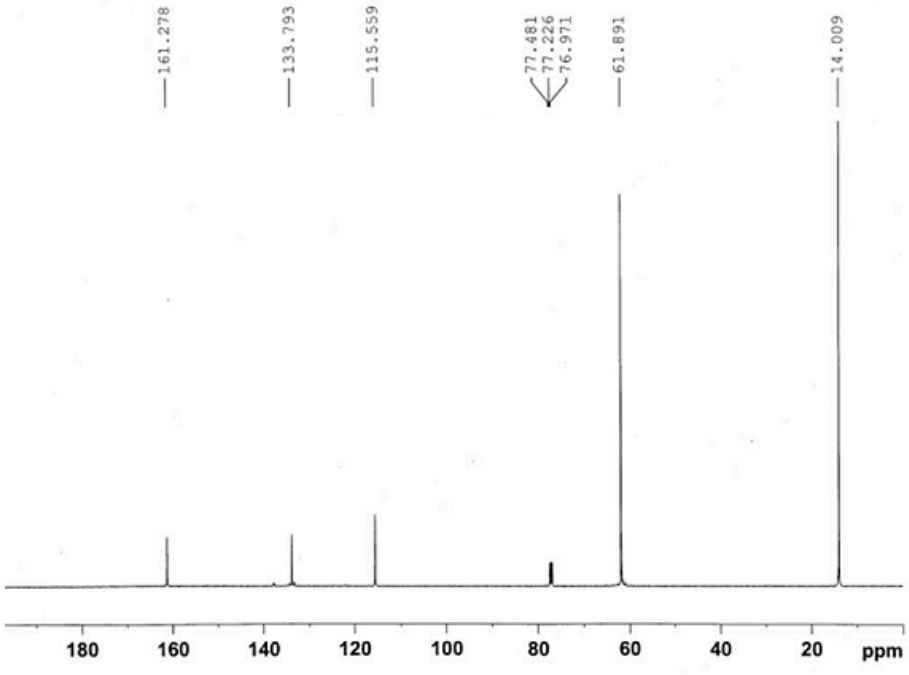

Figure S2: ^{13}C NMR spectrum of compound **4** in $CDCl_3$.

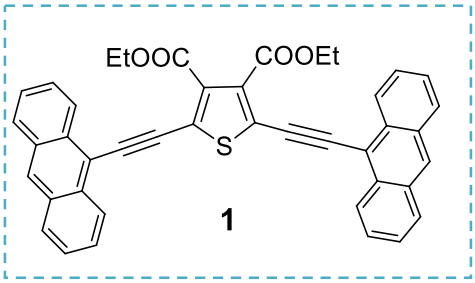

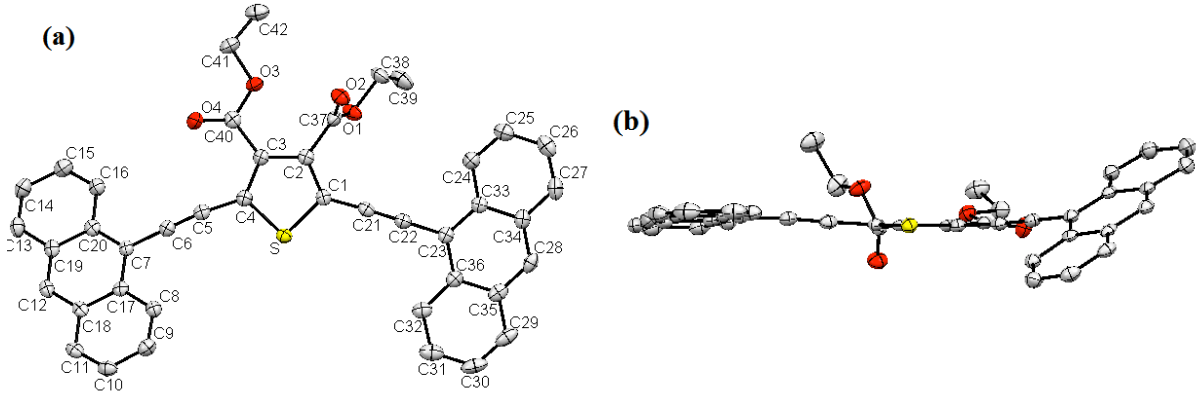

Figure S3: Crystal structure of compound **1** (a) front view and (b) side view.

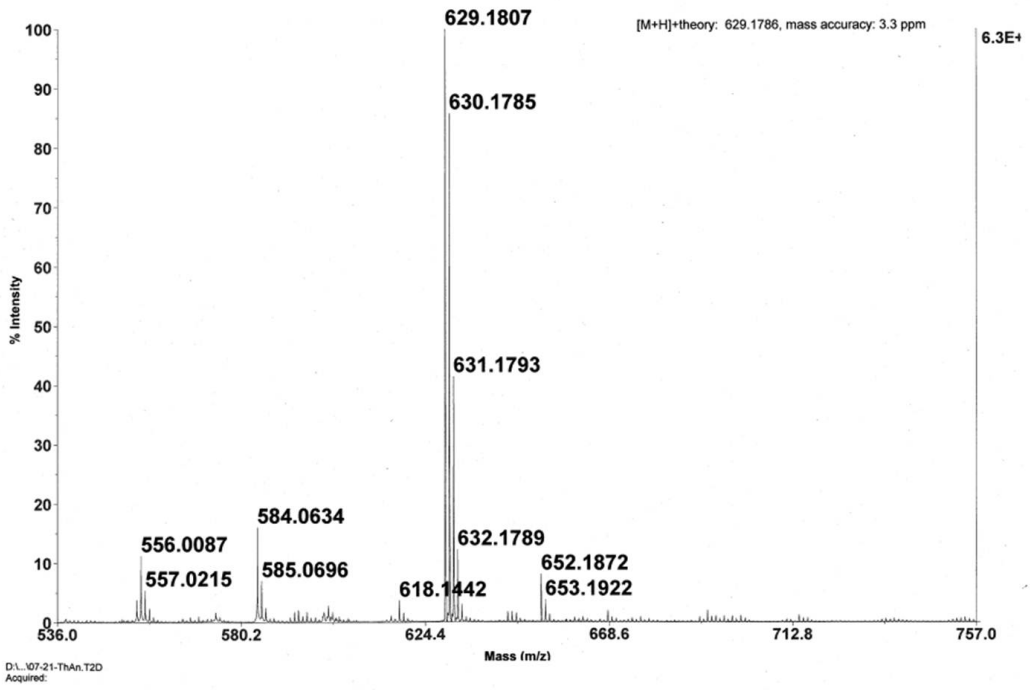

Figure S4: HR-MS mass spectrum of compound **1**.

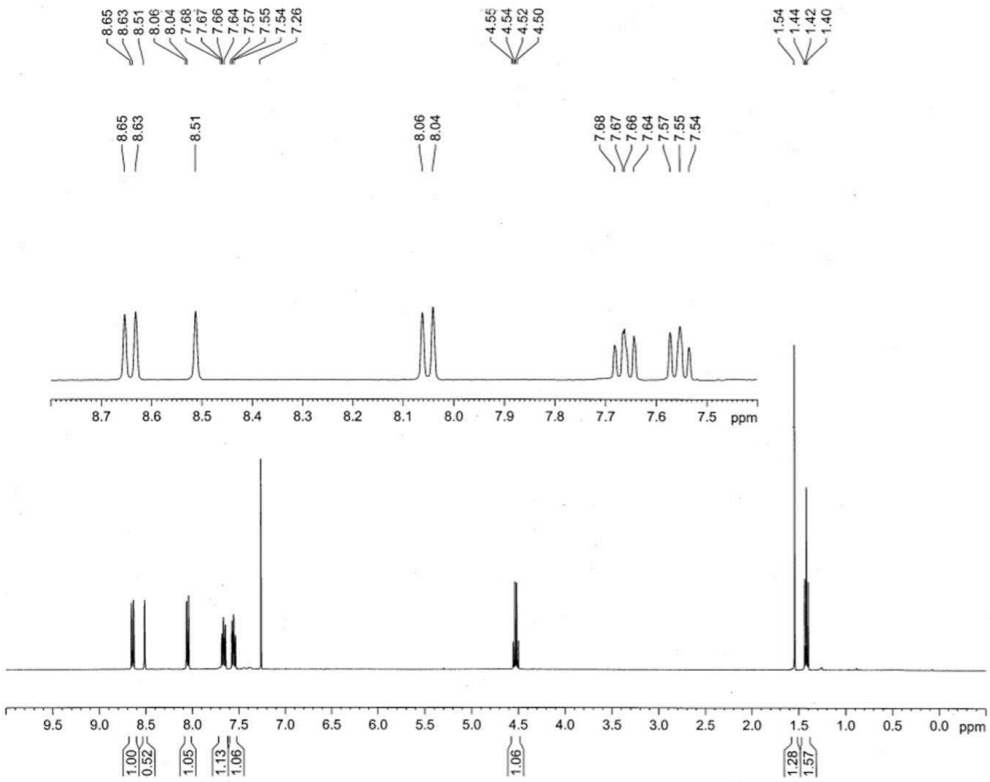

Figure S5: ^{1}H NMR spectrum of compound **1** in $CDCl_3$.

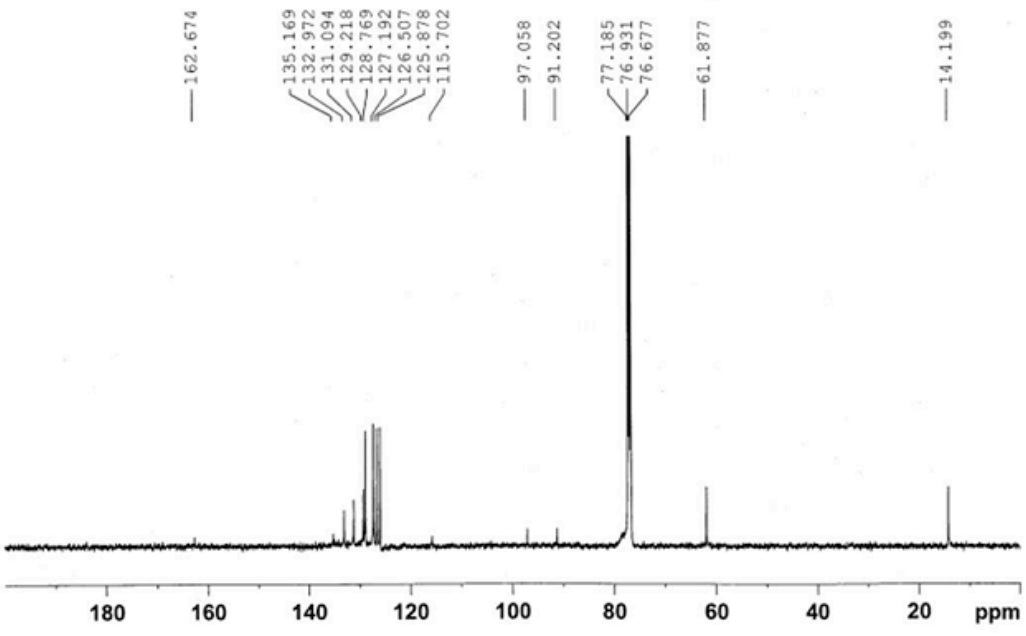

Figure S6: ^{13}C NMR spectrum of compound **1** in $CDCl_3$.

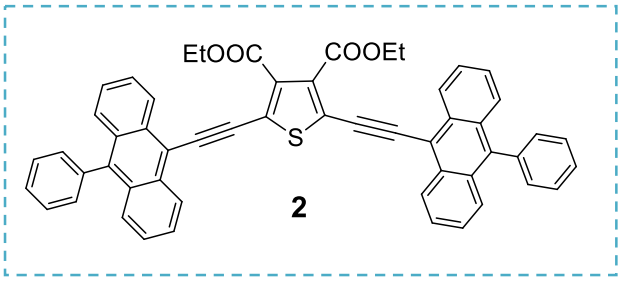

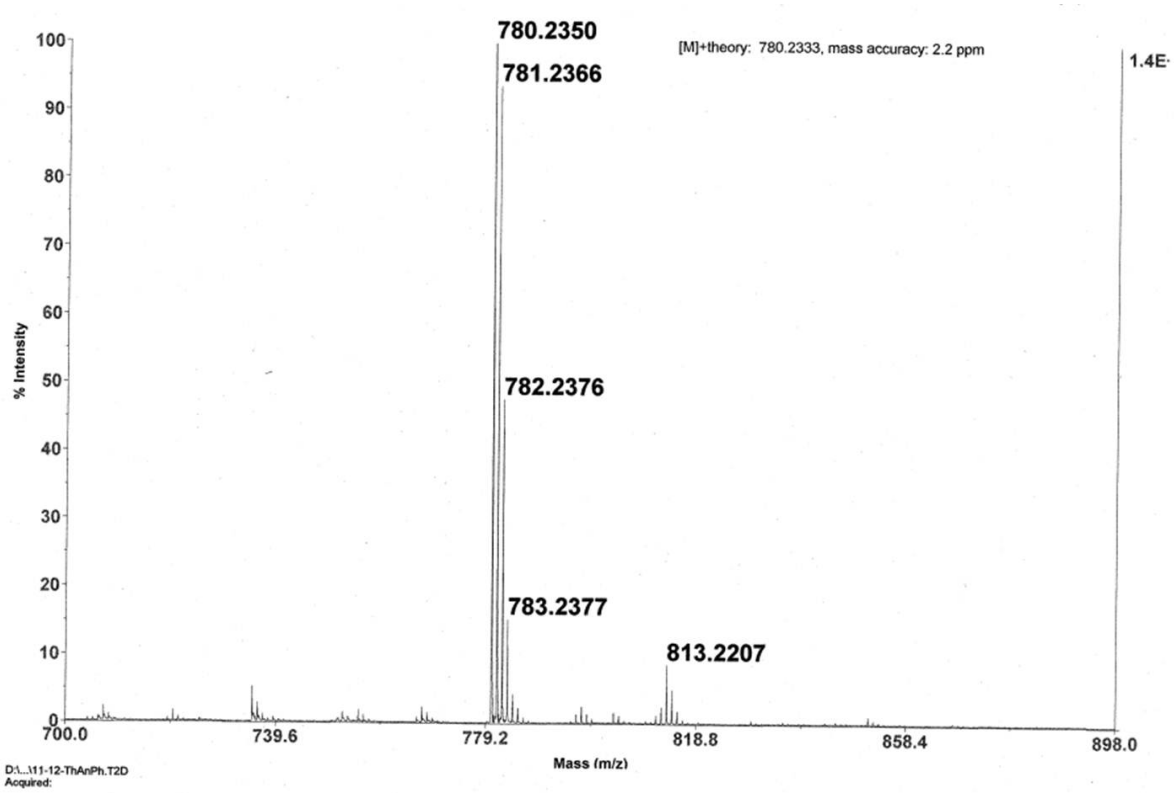

Figure S7: HR-MS mass spectrum of compound **2**.

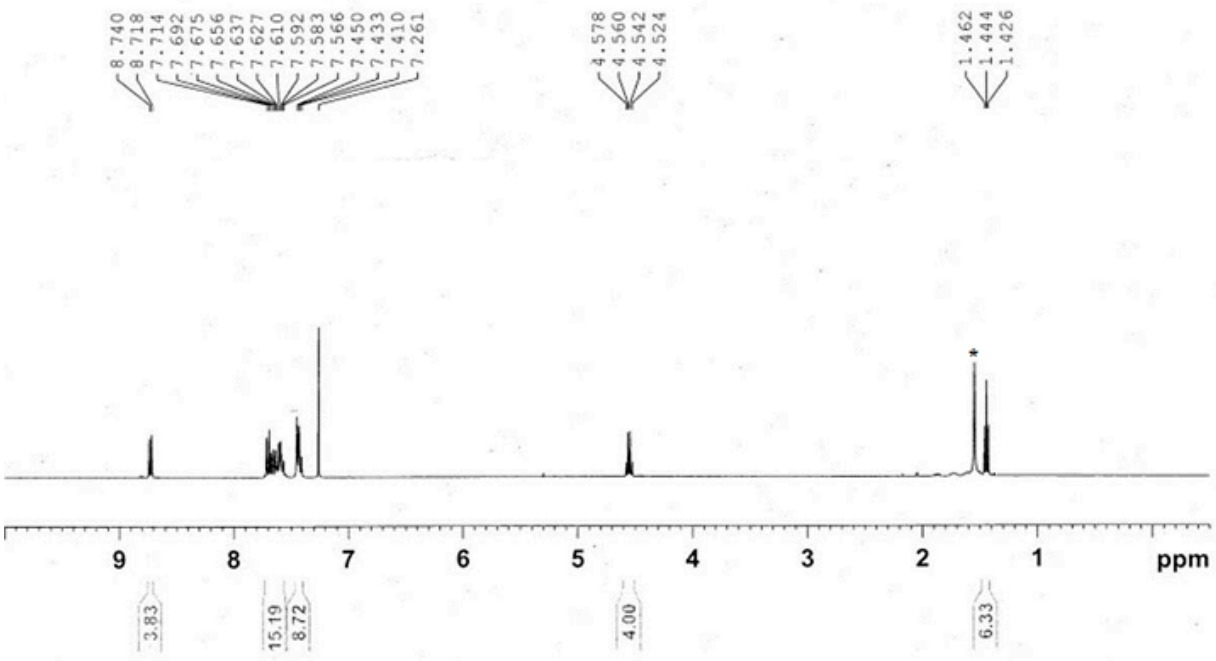

Figure S8: ^{1}H NMR spectrum of compound **2** in $CDCl_3$.

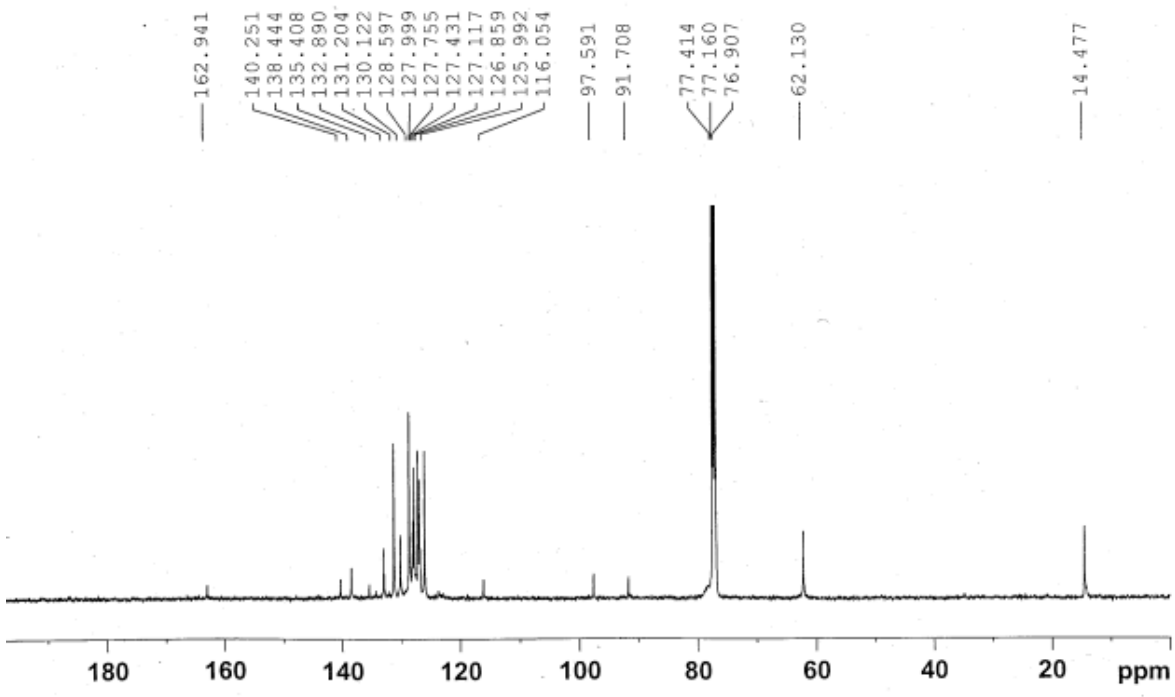

Figure S9: ^{13}C NMR spectrum of compound **2** in $CDCl_3$.

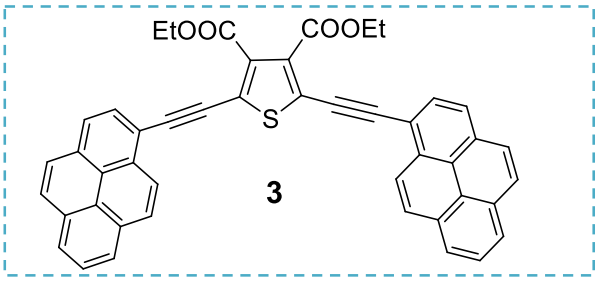

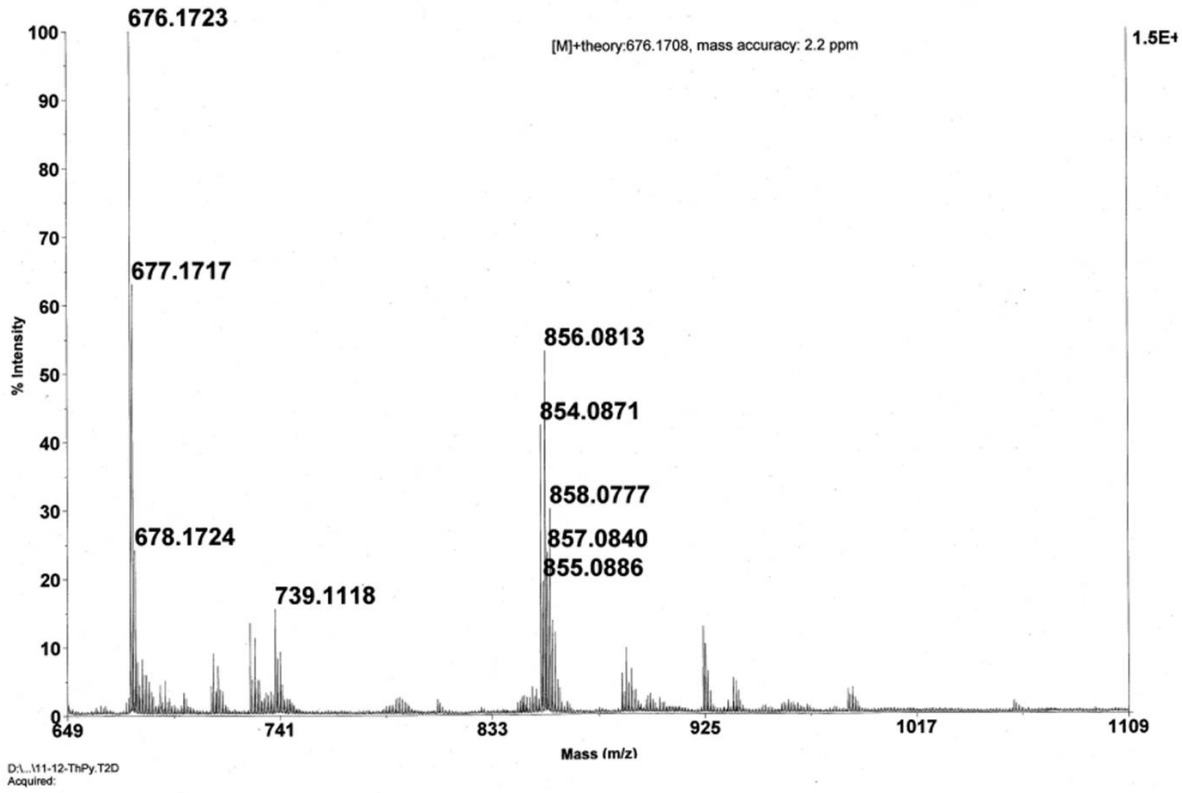

Figure S10: HR-MS mass spectrum of compound **3.**

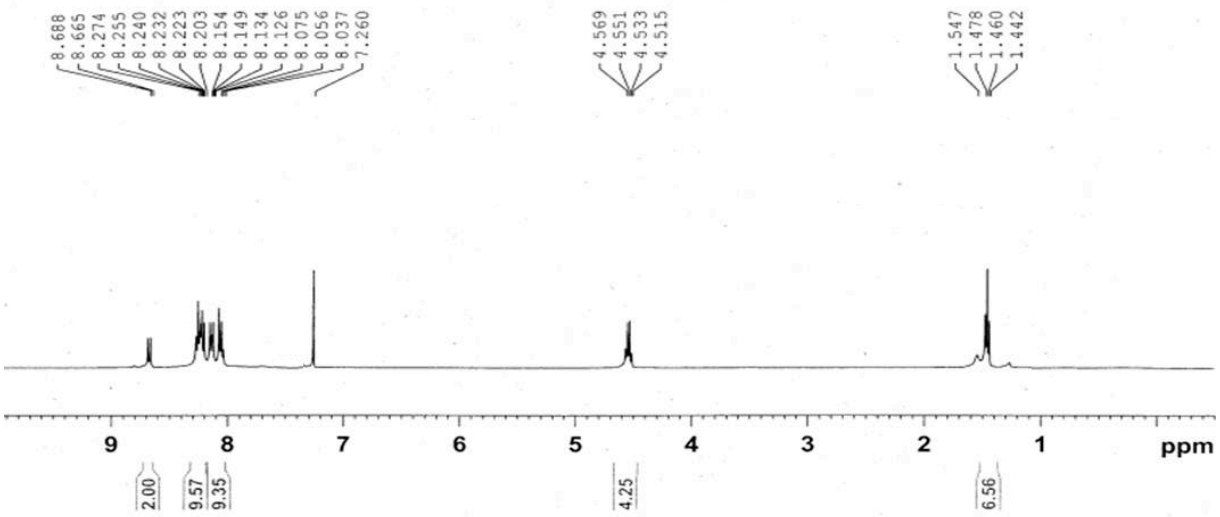

Figure S11: ^{1}H NMR spectrum of compound **3** in $CDCl_3$.

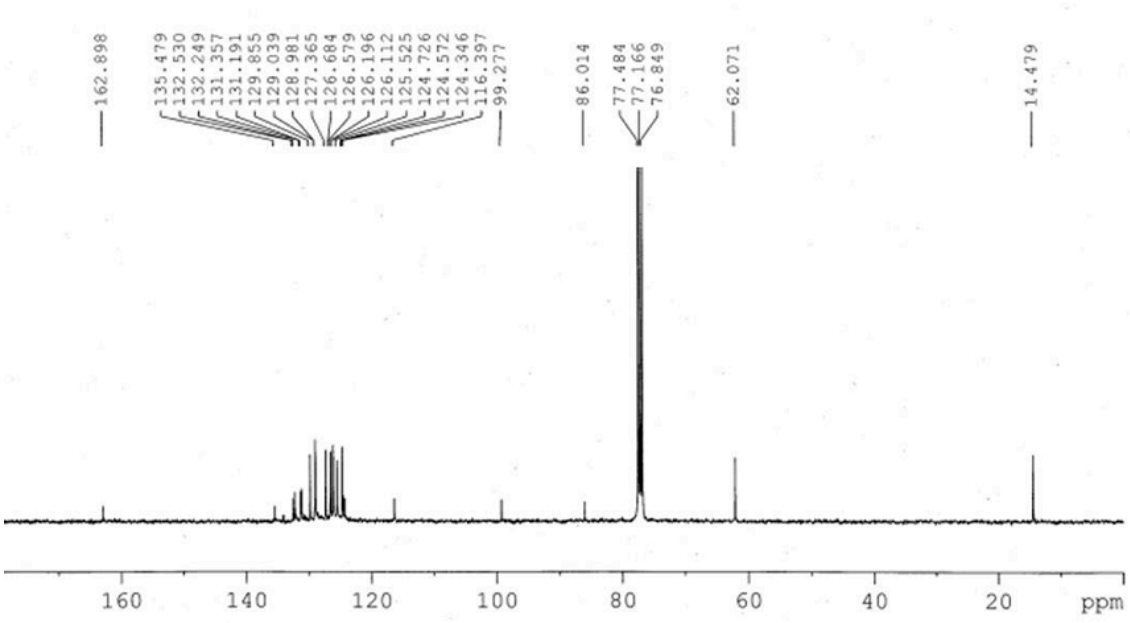

Figure S12: ^{13}C NMR spectrum of compound **3** in $CDCl_3$.

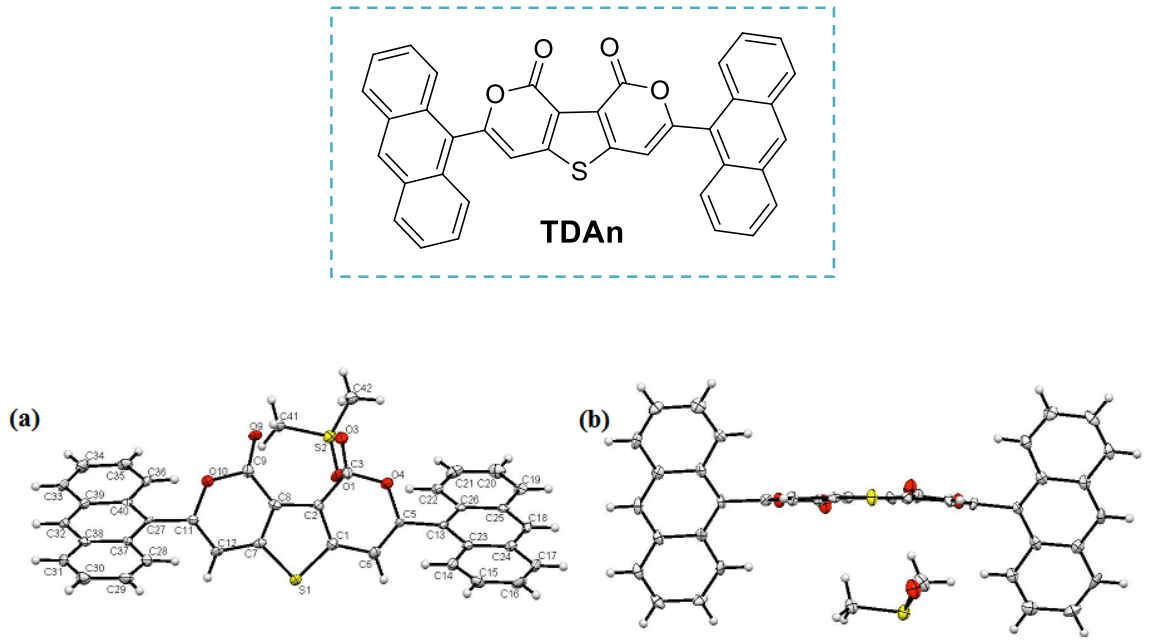

Figure S13: Crystal structure of compound **TDAn** in different views.

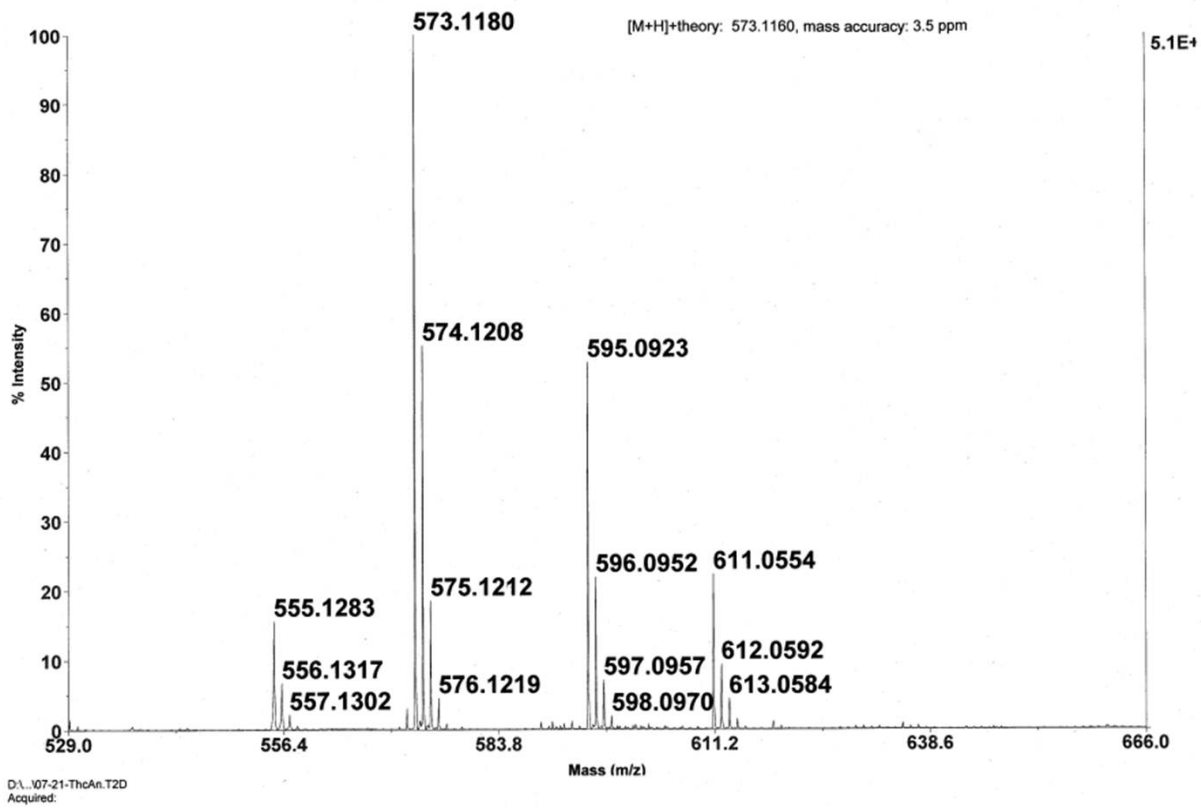

Figure S14: HR-MS mass spectrum of compound **TDAn**.

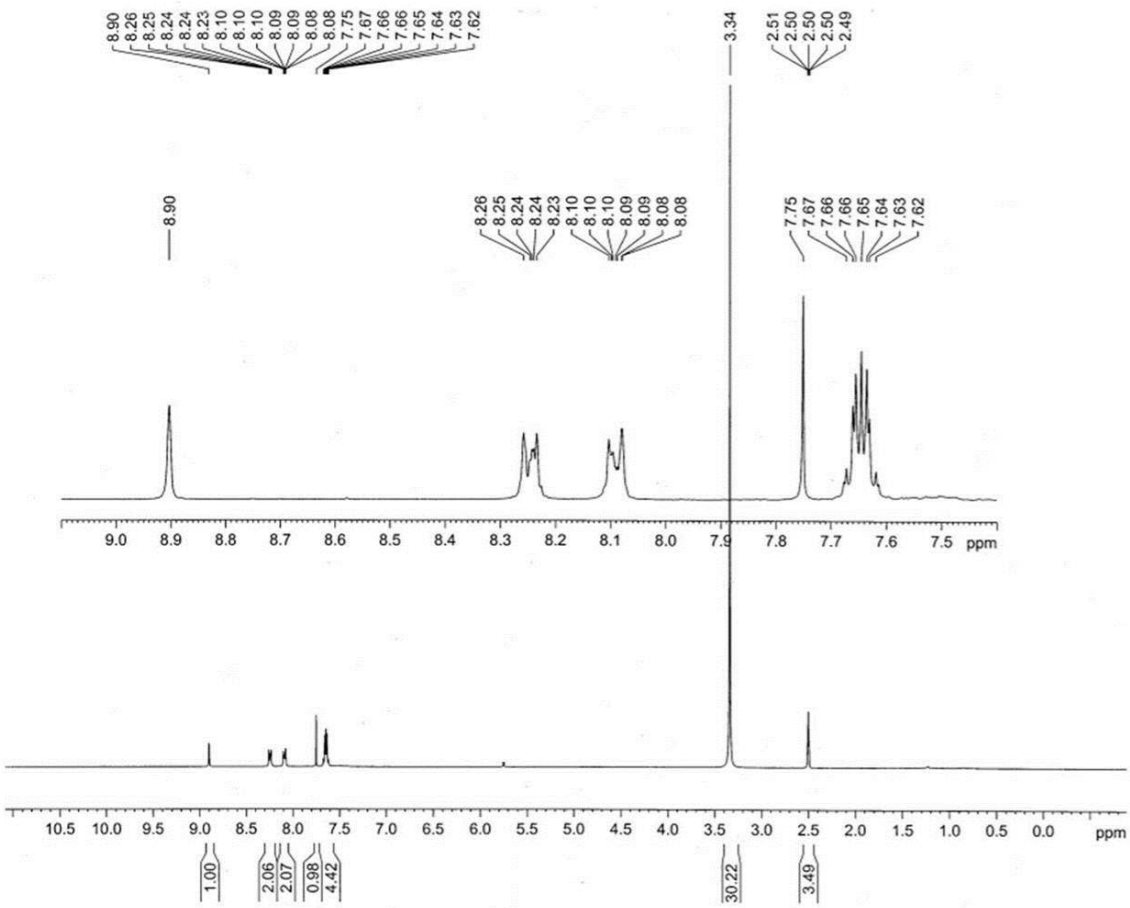

Figure S15: ^{1}H NMR spectrum of compound **TDAn** in [D_6]-DMSO.

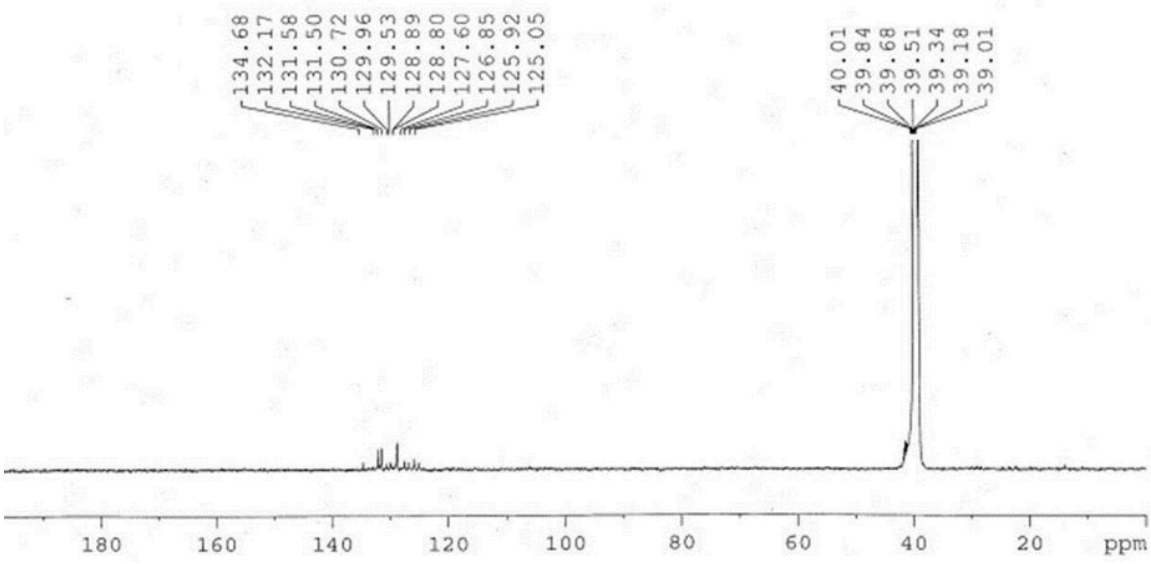

Figure S16: ^{13}C NMR spectrum of compound **TDAn** in [D_6]-DMSO.

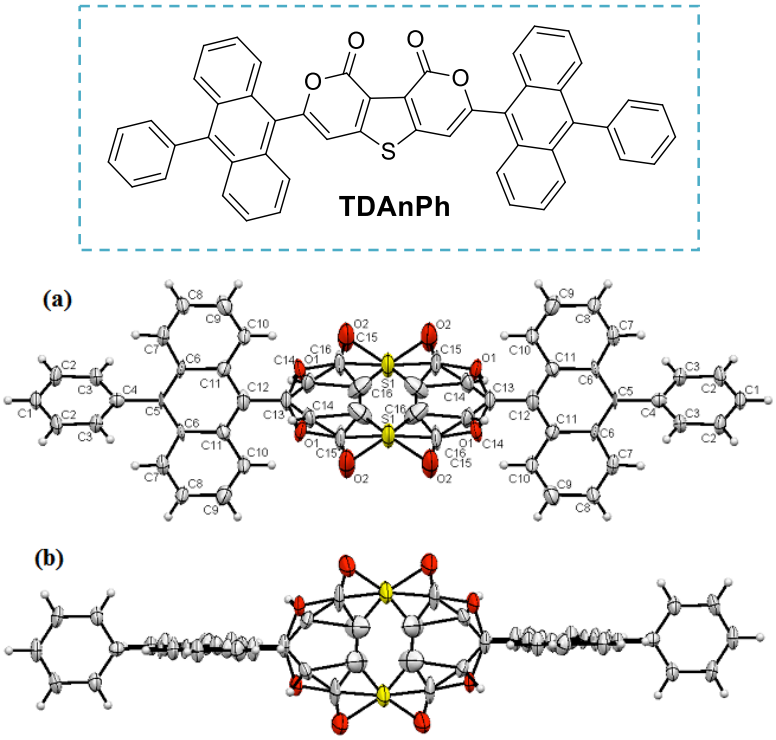

Figure S17: Crystal structure of compound **TDAnPh** in different views.

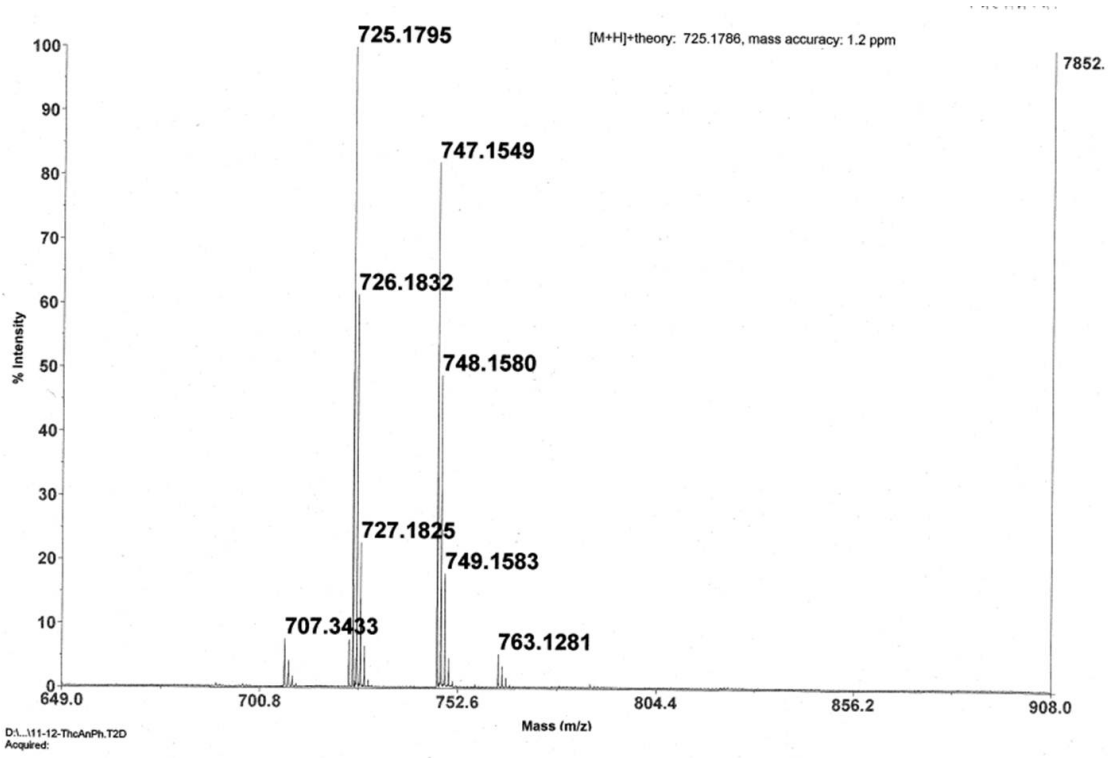

Figure S18: HR-MS mass spectrum of compound **TDAnPh**.

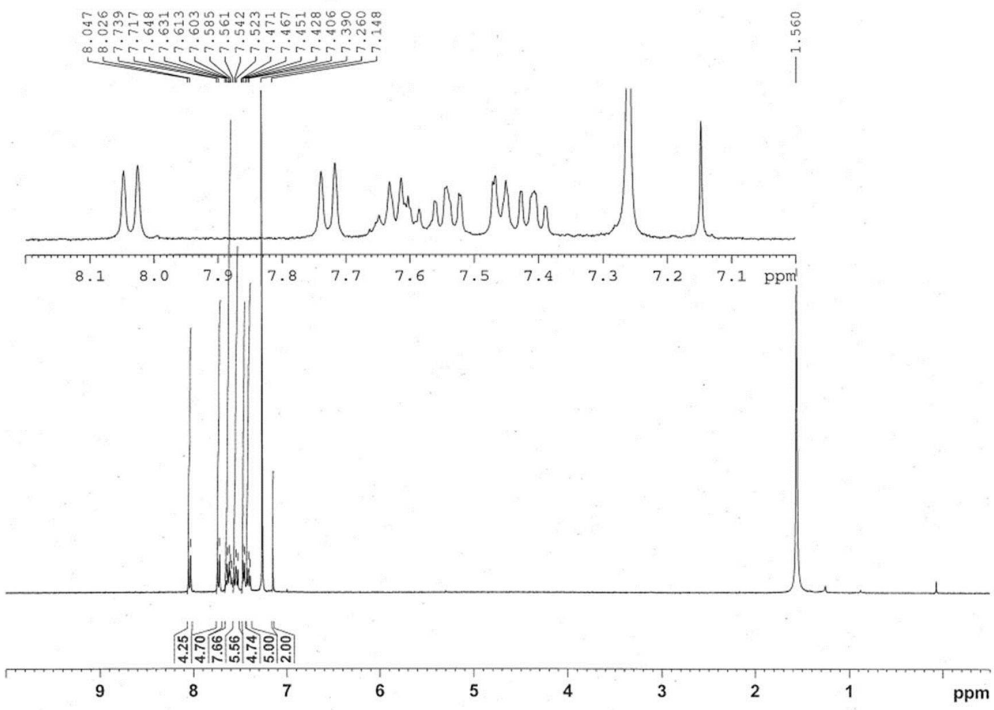

Figure S19: ^{1}H NMR spectrum of compound **TDAnPh** in $CDCl_3$.

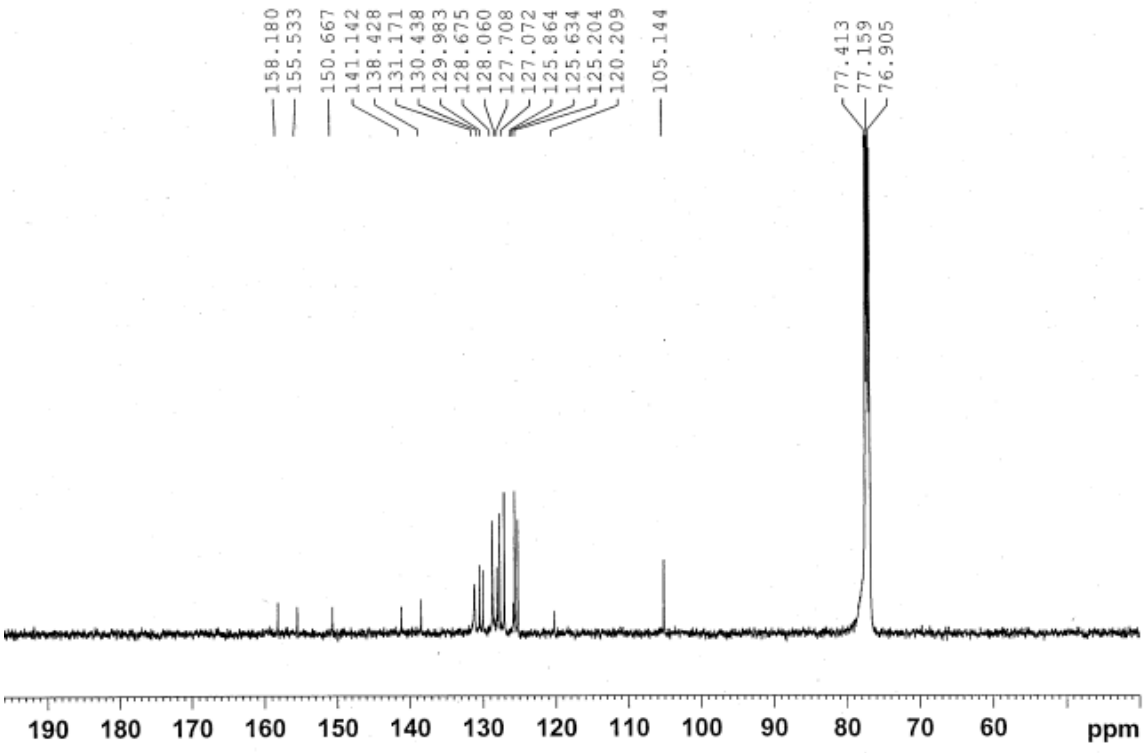

Figure S20: ^{13}C NMR spectrum of compound **TDAnPh** in $CDCl_3$.

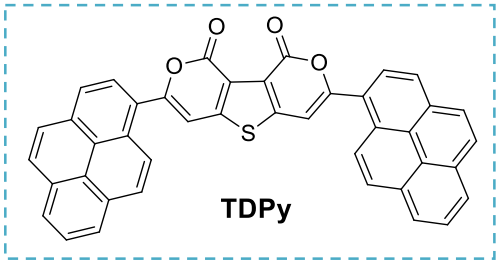

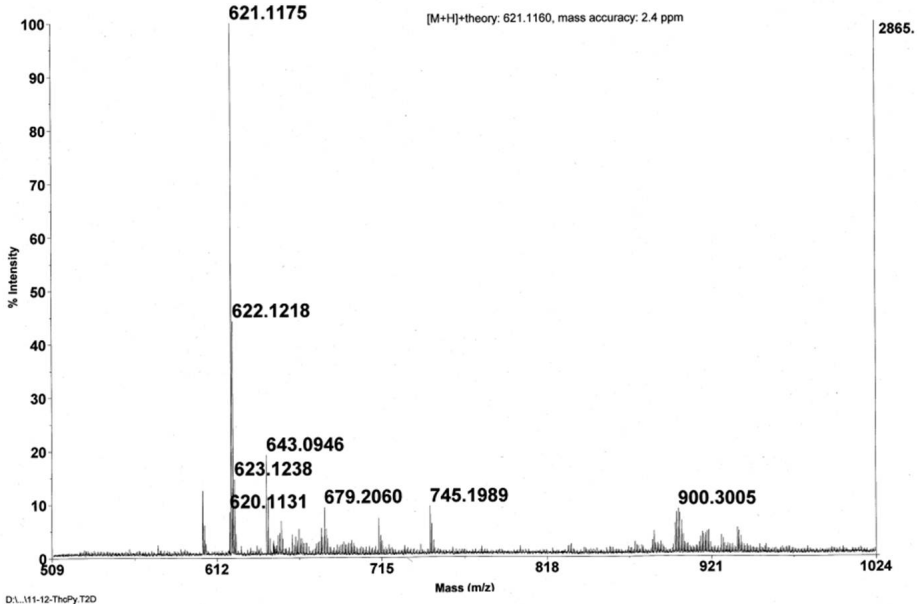

Figure S21: HR-MS mass spectrum of compound **TDPy**.

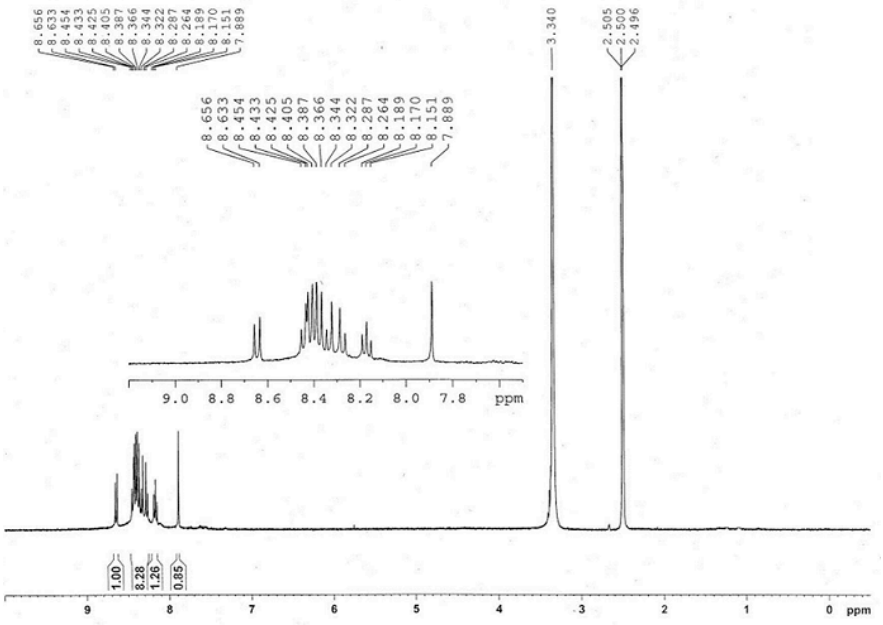

Figure S22: ^{1}H NMR spectrum of compound **TDPy** in [D_6]-DMSO.

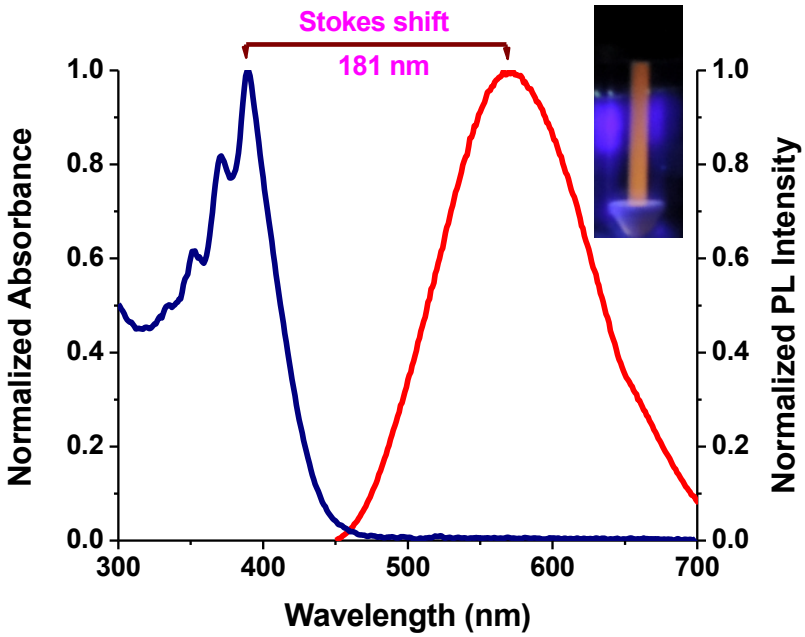

Figure S23: Normalized absorption (10^{-5} M) and PL (10^{-6} M) spectra of **TDAn** in toluene. Inset shows the colour of the compound under UV lamp (365 nm).

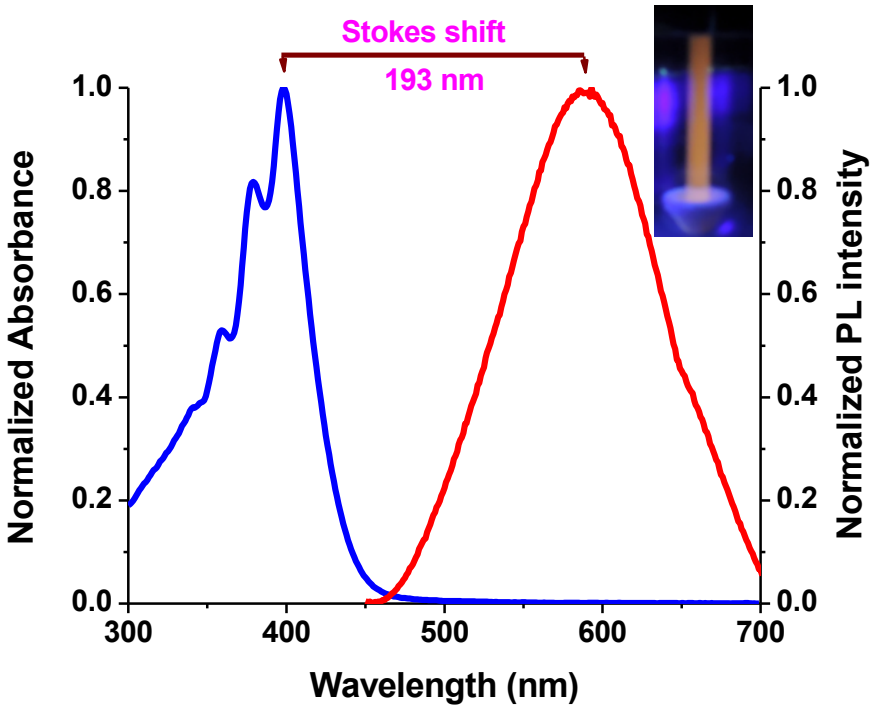

Figure S24: Normalized absorption (10^{-5} M) and PL (10^{-6} M) spectra of **TDAnPh** in toluene. Inset shows the colour of the compound under UV lamp (365 nm).

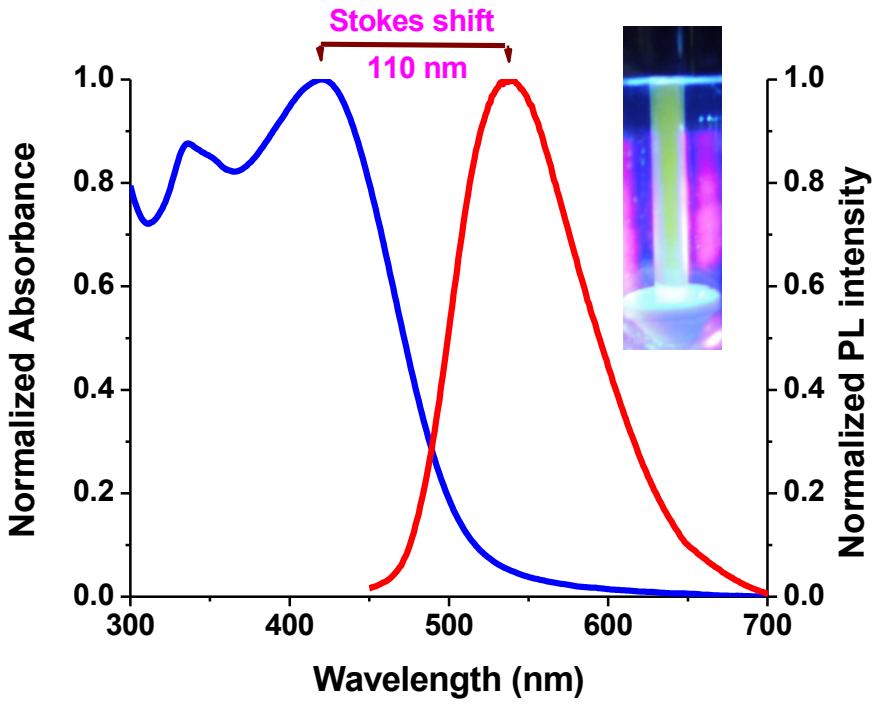

Figure S25: Normalized absorption (10^{-5} M) and PL (10^{-6} M) spectra of **TDPy** in toluene. Inset shows the colour of the compound under UV lamp (365 nm).

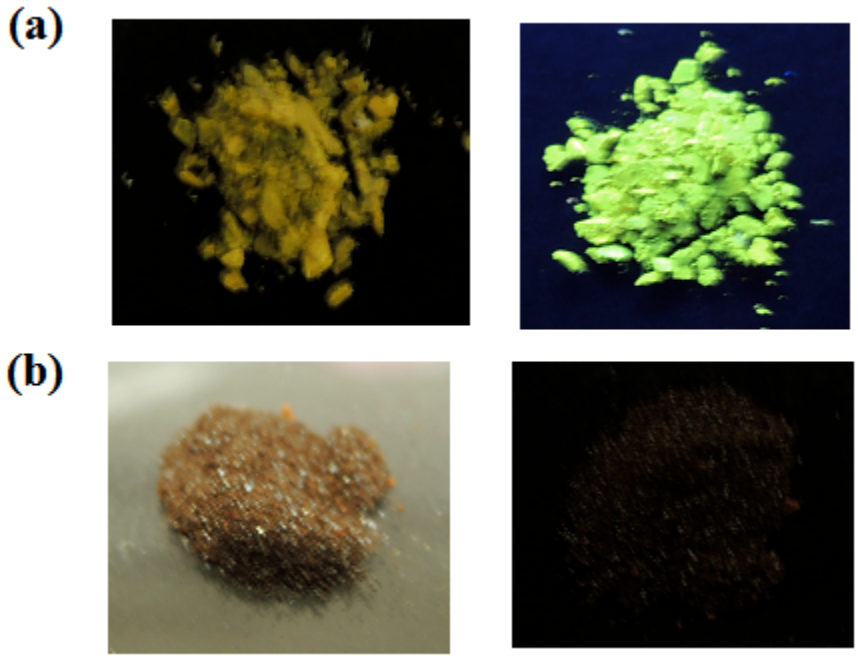

Figure S26: Photographs of **TDAnPh** (a) and **TDPy** (b) under ambient light (left) and UV-lamp (right).

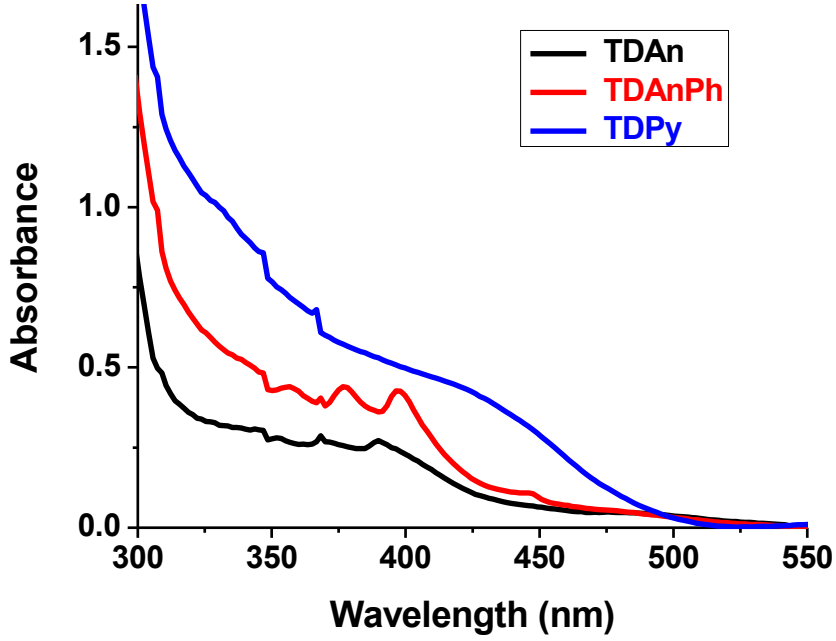

Figure S27: Comparison of absorption spectra of **TDAn**, **TDAnPh** and **TDPy** in 2-methyl THF at 77K ($5x10^{-6}$ M).

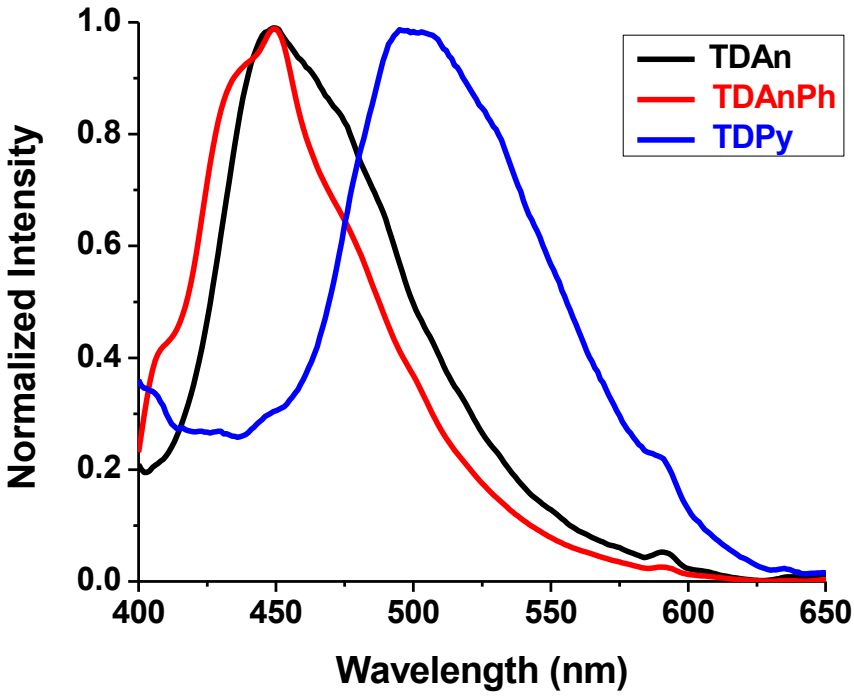

Figure S28: Comparison of PL spectra of **TDAn**, **TDAnPh** and **TDPy** in 2-methyl THF at 77K ($1x10^{-6}$ M).

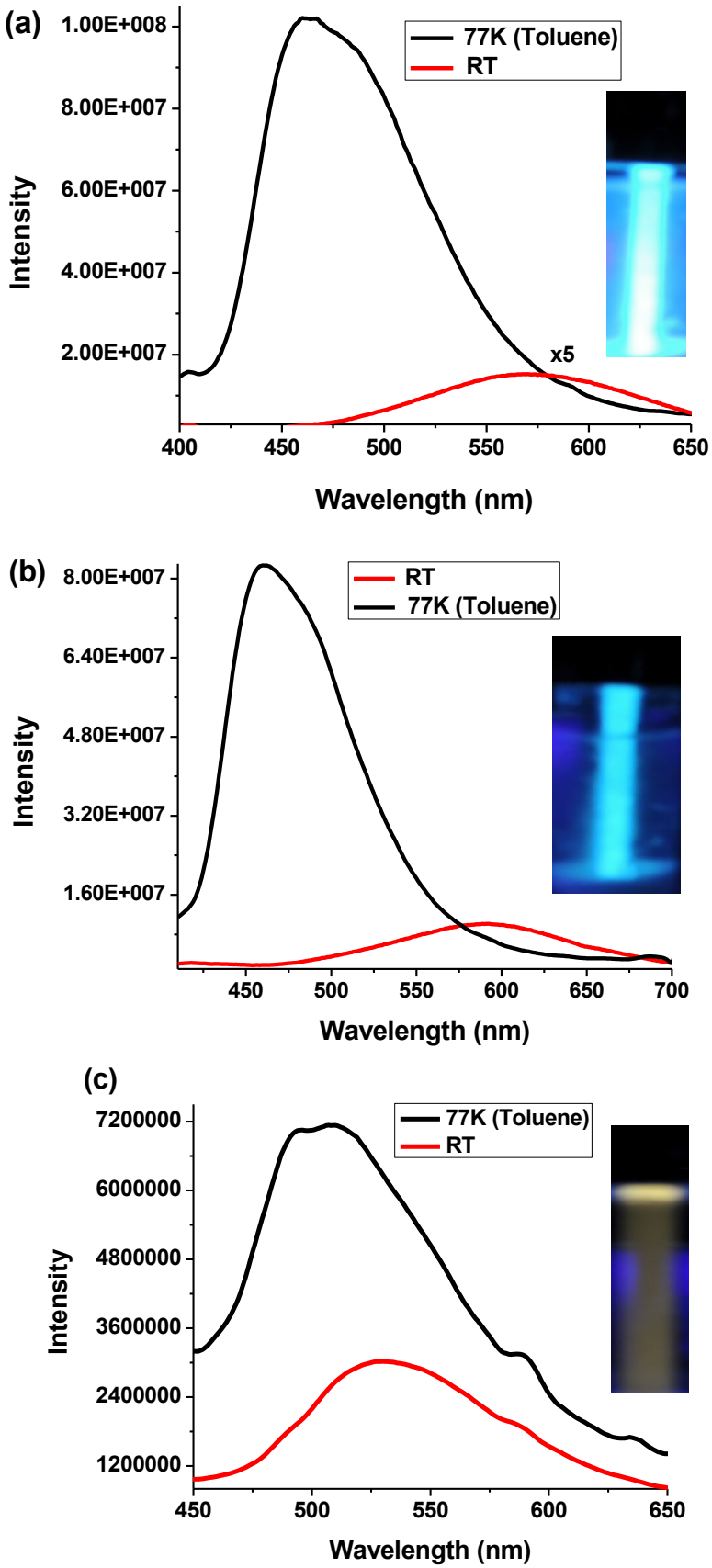

Figure S29: Comparison of PL spectra of (a) **TDAn**, (b) **TDAnPh** and (c) **TDPy** at room temperature and 77K ($5x10^{-6}$ M).

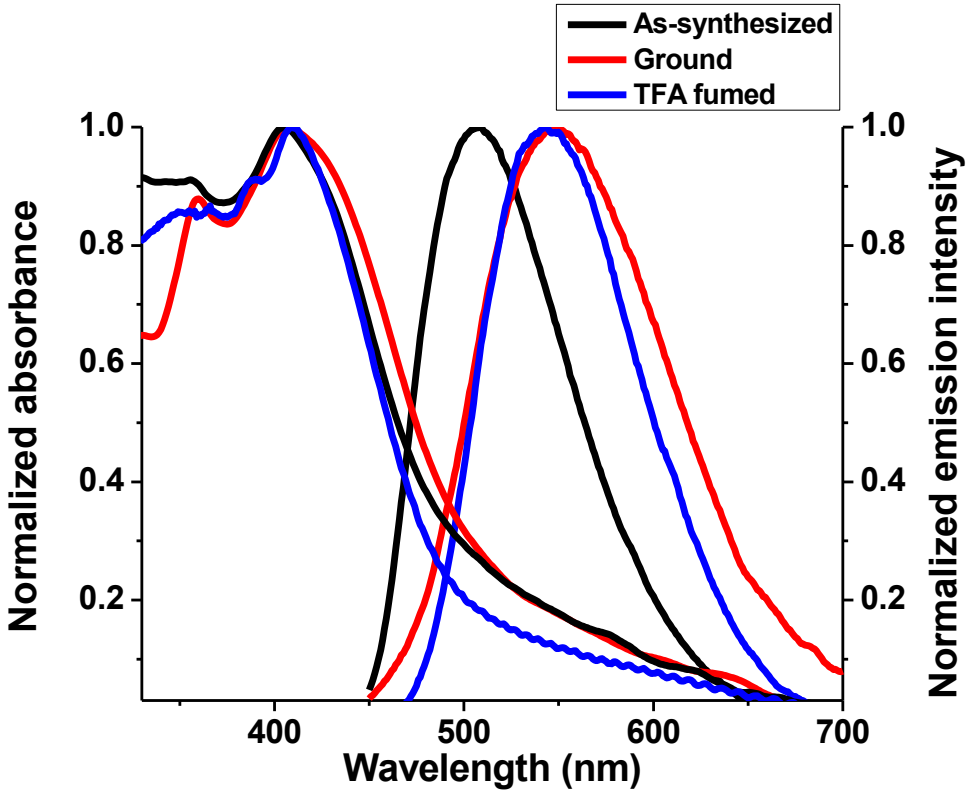

Figure S30: Solid-state absorption and emission spectra of **TDAn** in as-synthesized, ground and acid-fumed states.

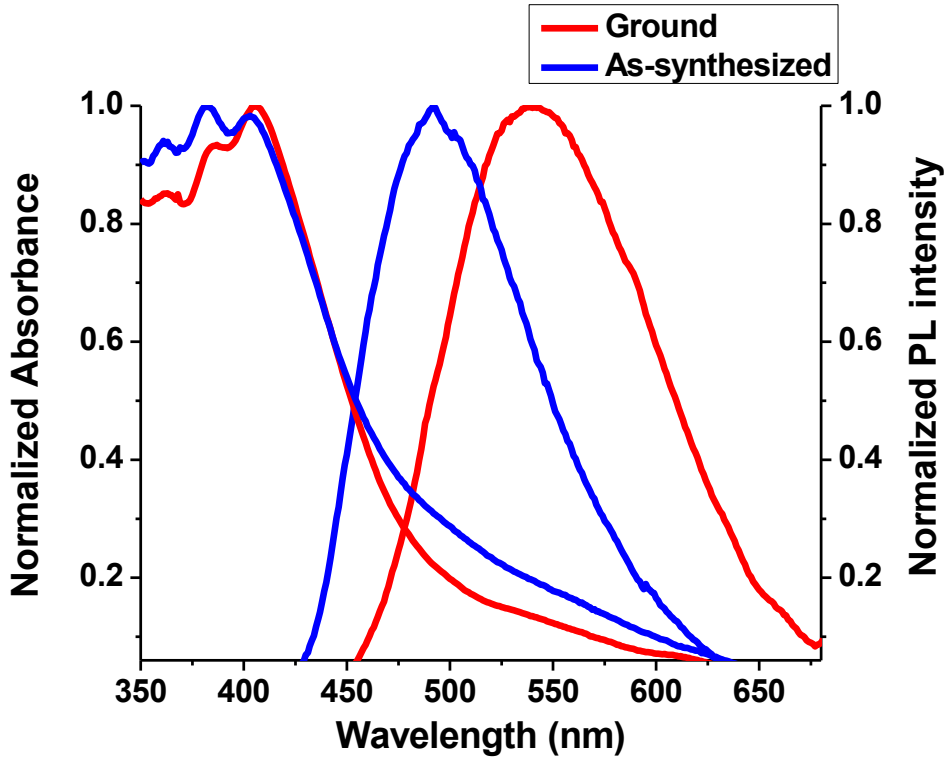

Figure S31: Solid-state absorption and emission spectra of **TDAnPh** in as-synthesized, ground states.

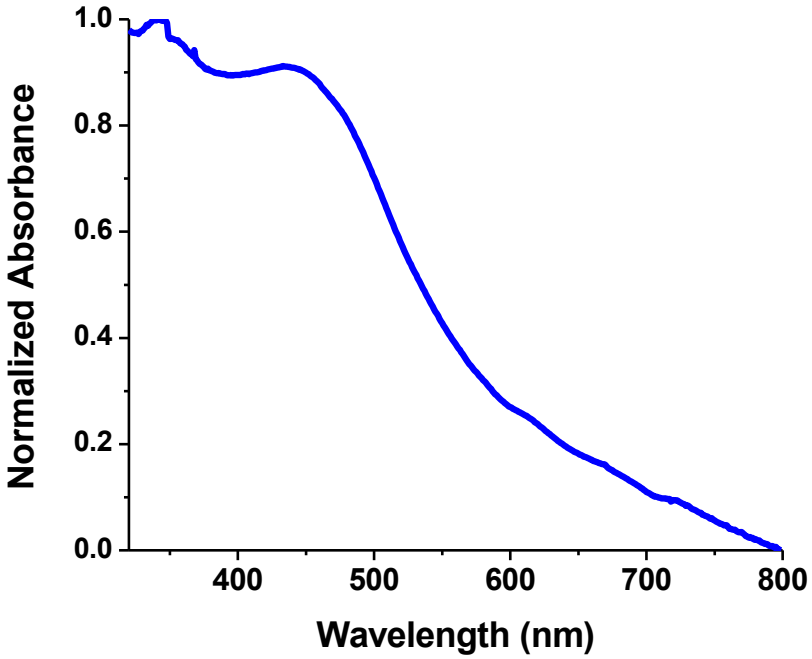

Figure S32: Solid-state absorption spectrum of **TDPy**.

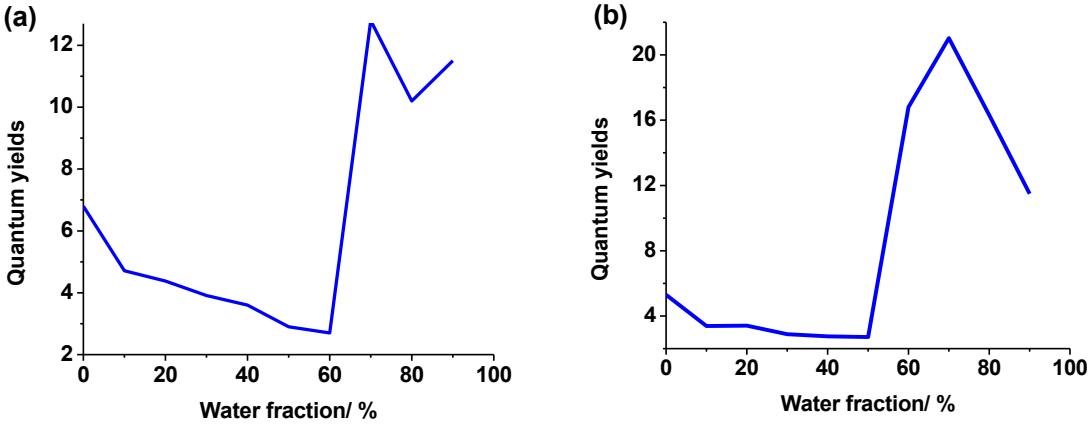

Figure S33: Change in quantum yields (ϕ) of (a) **TDAn** (b) **TDAnPh** in different THF/water fraction.

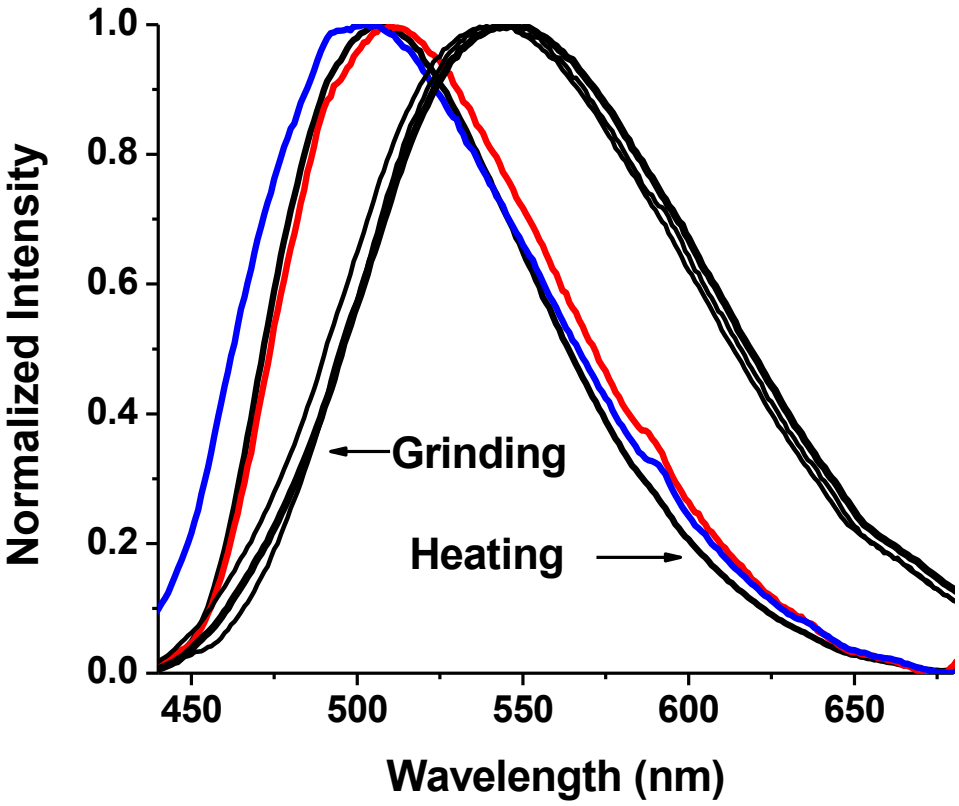

Figure S34: The normalized PL curves of **TDAn** reversible grinding and heating states

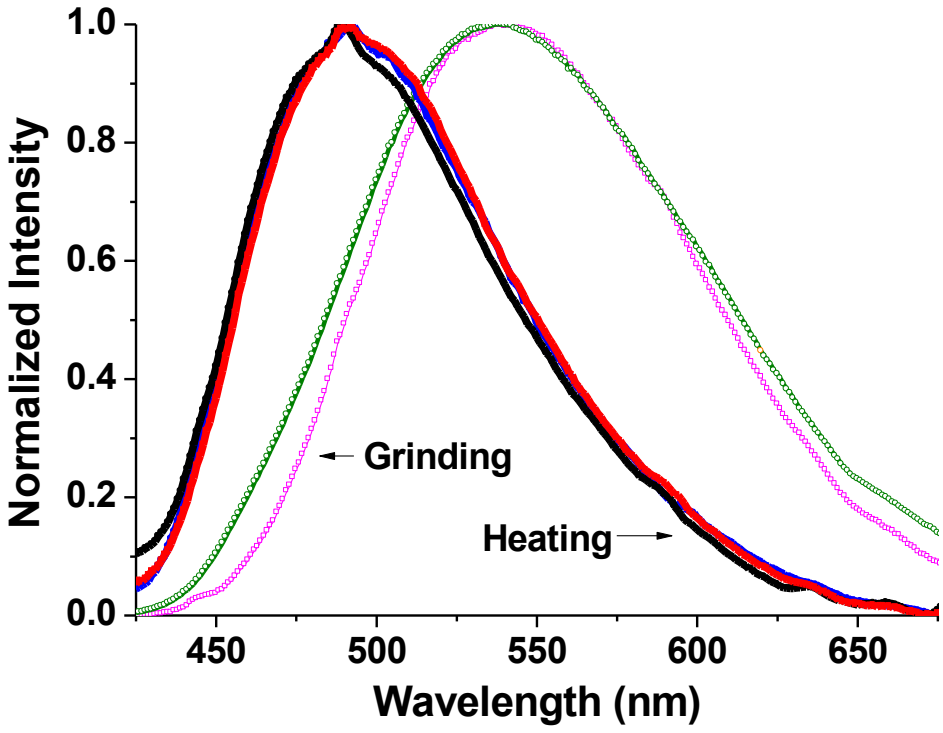

Figure S35: The normalized PL curves of **TDAnPh** reversible grinding and heating states

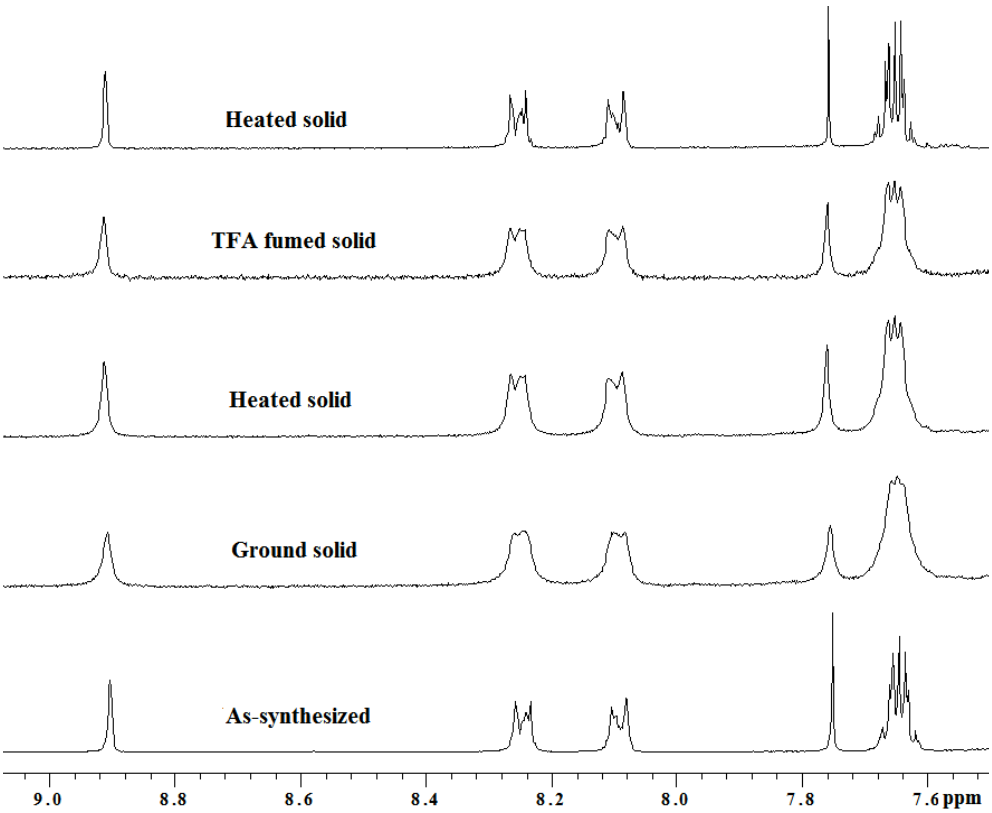

Figure S36: Comparison of ^{1}H NMR spectra of **TDAn** in various states.

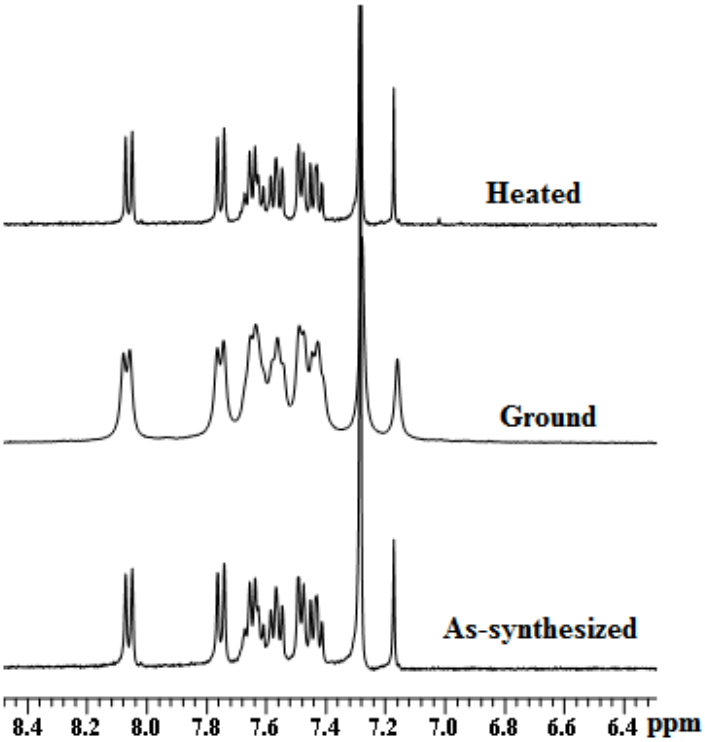

Figure S37: Comparison of ^{1}H NMR spectra of **TDAnPh** in various states.

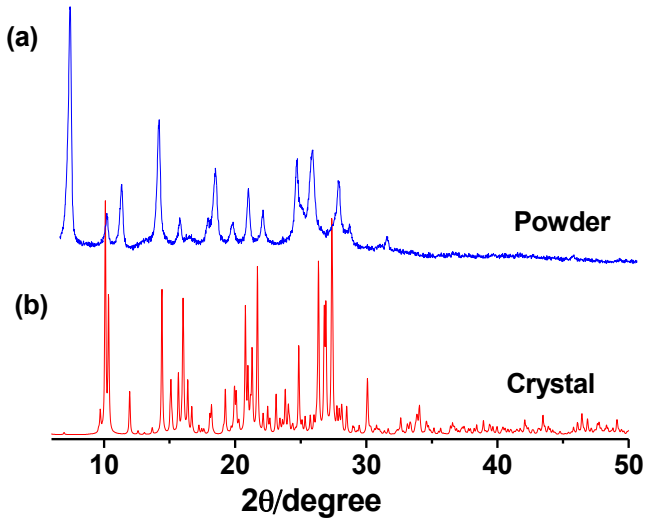

Figure S38: PXRD pattern of **TDAn**

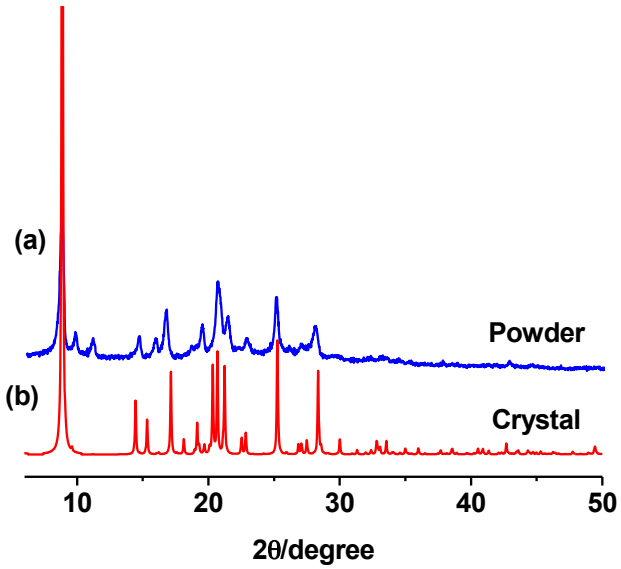

Figure S39: PXRD pattern of **TDAnPh**

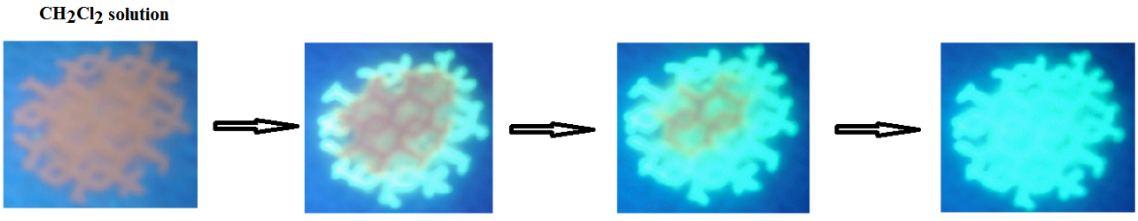

Figure S40: Photographs of **TDAnPh** in the process of evaporation of the solvent.

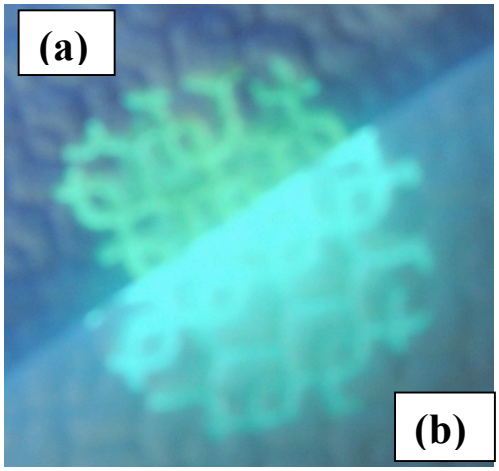

Figure S41: Solid sate emission colours of (a) **TDAn** and (b) **TDAnPh**.

Table S1: Photophysical data of **TDAn**, **TDAnPh** and **TDPy** in various solvents

	Solvent	λ_{abs} (nm)	λ_{em} (nm)	Quantum yields (ϕ)	Stokes shift (nm)
TDAn	Toluene	390	571	8.3	181
	$CHCl_3$	389	573	6.5	184
	THF	391	573	6.8	182
	2-MeTHF[a]	390	449	49	59
TDAnPh	Toluene	398	591	6.2	193
	$CHCl_3$	399	592	4.9	193
	THF	398	592	5.3	194
	2-MeTHF[a]	397	449	60	52
TDPy	Toluene	420	538	18.5	118
	$CHCl_3$	421	537	15.4	116
	THF	418	535	17.1	117
	2-MeTHF[a]	422	505	42	83

[a]Data collected at 77k

Table S2: Crystal Data and Structure Refinements of **TDAn** and **TDAnPh**

	TDAn	**TDAnPh**
formula	$C_{40}H_{26}O_5S_2$	$C_{30}H_{30}O_4S$
Formulawt	572.63	724.82
T, K	293 (2)	293 (2)
crystal system	monoclinic	monoclinic
space group	C 2/c	C 2/m
a, Å	36.933(5)	10.544(5)
b, Å	13.5190(17)	36.761(17)
c, Å	11.8390(13)	5.8903(19)
α,deg	90	90
β,deg	94.100(12)	101.277(16)
γ,deg	90	90
V,$Å^3$	5896.05	2239.05
Z	8	2
density, mg/m3	1.466	1.075
μ/mm^{-1}	0.231	0.112
θ range, deg	3.15 to 30.05°	2.05 to 25.11°
no. of reflcns collected	36817	7680
no. of unique reflcns		
R(int)	0.1992	0.1204
Goodness-of-fit on F^2	1.013	0.876
R1 [I > 2σ(I)]	0.0962	0.0834
wR2 [I > 2σ(I)]	0.1762	0.2048
R1 (all data)	0.2354	0.2180
wR2 (all data)	0.2348	0.2504

Computational Details

Geometry optimizations of the ground-state were done by density functional theory (DFT) employing the B3LYP functional and the 6-31G(d) basis set.[1,2]The frontier MO energy level distributions were estimated at the same functional level based on the optimized structures.

References

1. R. Ditchfield, W. J. Hehre, and J. A. Pople, "Self-Consistent Molecular Orbital Methods. IX. An Extended Extended Gaussian-type basis for molecular-orbital studies of organic molecules," *J. Chem. Phys.*1971, ***54*****,**724.

2. W. J. Hehre, R. Ditchfield, and J. A. Pople, "Self-Consistent Molecular Orbital Methods. XII. Further extensions of Gaussian-type basis sets for use in molecular-orbital studies of organic-molecules," *J. Chem. Phys.*1972, ***56***, 2257.

All calculations were performed with the Gaussian 09 program package:

Gaussian 09, Revision A.02, M. J. Frisch, G. W. Trucks, H. B. Schlegel, G. E. Scuseria, M. A. Robb, J. R. Cheeseman, G. Scalmani, V. Barone, B. Mennucci, G. A. Petersson, H. Nakatsuji, M. Caricato, X. Li, H. P. Hratchian, A. F. Izmaylov, J. Bloino, G. Zheng, J. L. Sonnenberg, M. Hada, M. Ehara, K. Toyota, R. Fukuda, J. Hasegawa, M. Ishida, T. Nakajima, Y. Honda, O. Kitao, H. Nakai, T. Vreven, J. A. Montgomery, Jr., J. E. Peralta, F. Ogliaro, M. Bearpark, J. J. Heyd, E. Brothers, K. N. Kudin, V. N. Staroverov, R. Kobayashi, J. Normand, K. Raghavachari, A. Rendell, J. C. Burant, S. S. Iyengar, J. Tomasi, M. Cossi, N. Rega, J. M. Millam, M. Klene, J. E. Knox, J. B. Cross, V. Bakken, C. Adamo, J. Jaramillo, R. Gomperts, R. E. Stratmann, O. Yazyev, A. J. Austin, R. Cammi, C. Pomelli, J. W. Ochterski, R. L. Martin, K. Morokuma, V. G.Zakrzewski, G. A. Voth, P. Salvador, J. J. Dannenberg, S. Dapprich, A. D. Daniels, Ö. Farkas, J. B. Foresman, J. V. Ortiz, J. Cioslowski, and D. J. Fox, Gaussian, Inc., Wallingford CT, 2009.